

The MPGD-Based Photon Detectors for the upgrade of COMPASS RICH-1

J. Agarwala, S. Dalla Torre, S. Dasgupta, M. Gregori, G. Hamar, S. Levorato, G. Menon, F. Tassarotto, Triloki, Y.X. Zhao

INFN Trieste, Trieste, Italy

F. Bradamante, A. Bressan, C. Chatterjee, P. Ciliberti, A. Martin

University of Trieste and INFN Trieste, Trieste, Italy

M. Alexeev, O. Denisov

INFN Torino, Torino, Italy

M. Chiosso

University of Torino and INFN Torino, Torino, Italy

D. Panzieri

University of East Piemonte, Alessandria and INFN Torino, Torino, Italy

C.D.R. Azevedo, J.F.C.A. Veloso

University of Aveiro, Aveiro, Portugal

M. Büchele, H. Fischer, F. Herrmann, S. Schopferer

Universität Freiburg, Freiburg, Germany

A. Cicuttin, M.L. Crespo

Abdus Salam ICTP, Trieste and INFN Trieste, Trieste, Italy

M. Finger, M. Finger Jr, M. Slunecka

Charles University, Prague, Czech Republic and JINR, Dubna, Russia

M. Sulc

Technical University of Liberec, Liberec, Czech Republic

E-mail: silvia.dallatorre@ts.infn.it

Abstract. After pioneering gaseous detectors of single photon for RICH applications using CsI solid state photocathodes in MWPCs within the RD26 collaboration and by the constructions for the RICH detector of the COMPASS experiment at CERN SPS, in 2016 we have upgraded

COMPASS RICH by novel gaseous photon detectors based on MPGD technology. Four novel photon detectors, covering a total active area of 1.5 m^2 , have been installed in order to cope with the challenging efficiency and stability requirements of the COMPASS physics programme. They are the first application in an experiment of MPGD-based single photon detectors. All aspects of the upgrade are presented, including engineering, mass production, quality assessment and performance.

Perspectives for further developments in the field of gaseous single photon detectors are also indicated.

1. Introduction

THE RICH-1 detector [1] of the COMPASS Experiment [2] at CERN SPS has been upgraded: four new Photon Detectors (unit size: $600 \times 600 \text{ mm}^2$), based on MPGD technology and covering a total active area of 1.5 m^2 replace the previously used MWPC-based photon detectors in order to cope with the challenging efficiency and stability requirements of the new COMPASS measurements. In fact, COMPASS goal is to deal with trigger rates up to $O(10^5) \text{ Hz}$ and beam rates up to $O(10^8) \text{ Hz}$. Concerning increased stability, this is provided by the new detector architecture, as explained in the following. In COMPASS RICH-1, MPGD photon detectors are used for the first time in a running experiment. This realization also opens the way of a more extended use of novel gaseous photon detectors in the domain of the Cherenkov imaging technique for Particle IDentification (PID), key detectors in several research sectors and, in particular, in hadron physics. The relevance is related to the role of gaseous photon detectors, which are still the only available option to instrument detection surfaces when insensitivity to magnetic field, low material budget, and affordable costs in view of large detection systems are required. The MPGD-based photon detectors overcome the limitation of the previous generation of gaseous photon detectors thanks to two essential performance characteristics: reduced ion and photon backflow to the photocathode, namely reduced ageing and increased electrical stability, and faster signal development, namely higher rate capabilities.

2. The novel photon detectors

The detector architecture is the result of a seven-year R&D activity [3]. It is based on a hybrid MPGD combination (Fig. 1), consisting in two layers of THick GEMs (THGEM) [4] followed by a resistive MicroMegas (MM) [5] on a pad segmented anode. The first THGEM also acts as a reflective photocathode: its top face is coated with a CsI film. The feedback of photons generated in the multiplication process is suppressed by the presence of two THGEM layers, while the large majority of the ions from multiplication are trapped in the MM stage. MPGD properties ensure signal development in about 100 ns.

Each of the four large ($600 \times 600 \text{ mm}^2$) single photon detectors is formed by two identical modules $600 \times 300 \text{ mm}^2$, arranged side by side. The THGEM geometrical parameters are: $470 \text{ }\mu\text{m}$ thickness, $400 \text{ }\mu\text{m}$ hole diameter and $800 \text{ }\mu\text{m}$ pitch. Holes are rim-less, namely there is no uncoated area around the hole edge. They are arranged in a regular pattern with equilateral triangles as elementary cell. In order to mitigate the effect of occasional discharges, the top and bottom electrodes of each THGEM are segmented in 12 parallel areas separated by 0.7 mm clearance, each biased via an individual protection $500 \text{ M}\Omega$ resistor. Therefore, discharges only affect a single sector and the operating conditions are restored in about 10 s. The two layers are staggered, namely there is complete misalignment between the two set of holes: it is so possible to enlarge the electron cloud reaching the MM stage, therefore favoring larger gain in the last amplification stage.

The MMs have a gap of $128 \text{ }\mu\text{m}$; they are built by the MM bulk technology [6] using $300 \text{ }\mu\text{m}$ diameter pillars with 2 mm pitch. The MM anode is segmented in $7.5 \times 7.5 \text{ mm}^2$ pads. The MM

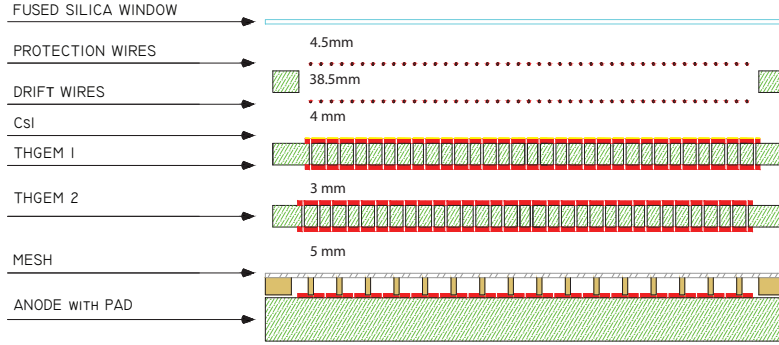


Figure 1. Sketch of the hybrid single photon detector: two staggered THGEM layers are coupled to a resistive bulk MM. Image not to scale.

resistivity is realized through an original implementation, where no resistive layer is applied to the pads: the resistivity is obtained by $470\text{ M}\Omega$ resistors in series with each individual pad (Fig. 2). The 0.5 mm clearance between pads prevents the occasional discharges to propagate towards the surrounding pads: the voltage drop of the anodic pads surrounding a tripping one is about 2 V over the typical 600 V operation voltage, causing a local gain drop lower than 4% . The nominal voltage condition of the pad where the discharge occurred is restored in about 1 s . The detector is operated with $\text{Ar:CH}_4 = 50:50$ gas mixture, which ensures effective extraction of photoelectrons from the photocathode. The typical voltage applied are 1270 V across THGEM1, 1250 V across THGEM2, and 620 V to bias the MM. The drift field above the first THGEM is 500 V/cm , the transfer field between the two THGEMs is 1000 V/cm and the field between the second THGEM and the MM micromesh is 1000 V/cm . The effective gain-values for the three multiplication layers are around 12, 10 and 120; these values include the electron transfer efficiency.

The novel detectors are read out by the read-out system already used for the MWPCs with CsI photocathode. This read-out system is based on the APV front-end chip [7] read out by a dedicated ADC [8].

3. Construction, quality control of the components, assembly and installation

The electrical stability of large-size THGEMs is a critical issue. A dedicated protocol has been elaborated for finishing the industrial produced THGEMs [9]. It includes polishing with fine grain pumice powder, cleaning with water at high pressure, ultrasonic bath with Sonica PCB solution (PH11), rinsing with distilled water and backing in oven at 160°C . The procedure moves THGEM breakdown voltage to at least 90% of the phenomenological Paschen limit [10]. The quality control of the detector components includes:

- the preselection of the raw material for the PCB that will form the THGEMs in order to use only foils with homogeneous thickness to guarantee the homogeneity of the gain;
- the THGEM control by optical inspection, by collecting and analyzing microscope images, scanning by samples the large multiplier surface;
- the THGEM validation by gain maps using the multipliers in single layer detectors; gain uniformity at 7% r.m.s. is obtained;

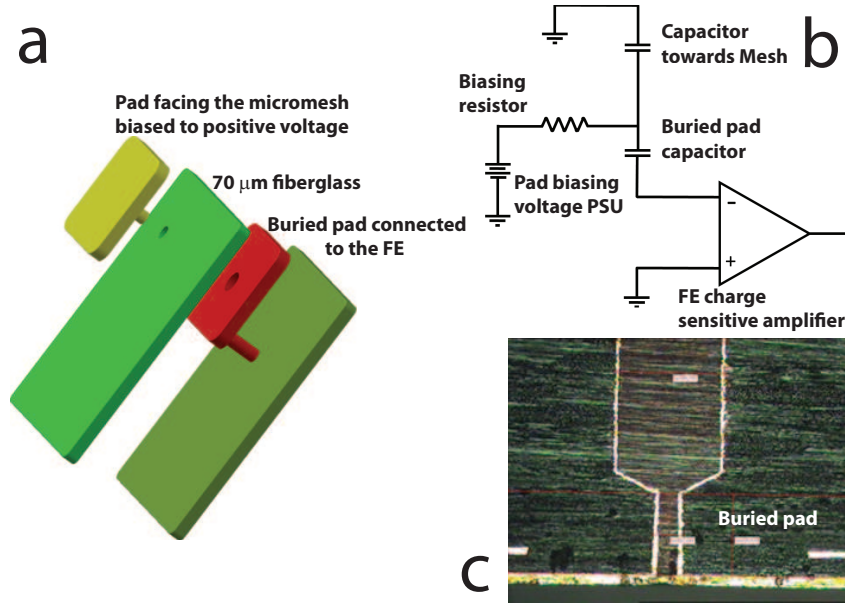


Figure 2. a) Sketch of the capacitive coupled readout pad. The biasing voltage is distributed via independent $470\text{ M}\Omega$ resistors to the pad facing the micromesh structure (yellow pad in the sketch). The buried pad (red pad in the sketch) is isolated via $70\text{ }\mu\text{m}$ thick fiberglass and connected to the front end chip. b) Schematic of the capacitive coupled pad principle illustrated via discrete element blocks. c) Metallography section of the PCB: detail of the through-via connecting the external pad through the hole of the buried pad. The reduced diameter of the through-via reaching the external pad contributes preserving the pad planarity.

- the collection of MM gain maps illuminating the detectors by an X-ray gun station; gain uniformity at 5% r.m.s. is obtained;
- the measurement of the quantum efficiency of the CsI photocathodes, which is performed immediately after the coating process; the uniformity within a photocathode is at the 3% level r.m.s. and among the whole production at the 10% level r.m.s.;
- the gas leak checks and overall electrical stability checks of the final detectors.

CsI photocathodes must never be exposed to air to fully preserve their quantum efficiency: in fact, CsI is highly hygroscopic and it reacts with water vapour that decomposes the molecule. Therefore, the presence of CsI photocathodes imposes to perform detector assembly, transportation and installation in glove boxes flushed with N_2 .

4. The high voltage system

An essential tool for the detector commissioning is the High Voltage (HV) control system, which also allows for voltage and current monitoring and data logging. The power supplies are commercial ones by CAEN inserted in a SY4527 mainframe. A1561HDN units power the THGEMs, while A7030DP power supplies are used for the MMs. The four detectors are organized, from the HV supply point of view, in four independent sectors each; nine different electrode types, each one with its specific role, are present in the multilayer detectors. The total number of HV channels is 136. Manual setting and control of all these HV channels would be both unpractical and unsafe. The voltages and currents of all the channels are read-out and recorded at 1 Hz frequency. If the current spark rate is above a given value the voltage is automatically readjusted. The system also provides automatic voltage adjustment to compensate for the

variation of the environmental parameters, namely pressure and temperature, that can affect the detector gain. Gain stability at the 5% level over months of operation has been obtained.

5. Preliminary performance results

The novel detectors have been used during COMPASS runs in year 2016 and 2017, for a total running period of about 12 months at COMPASS nominal beam rates. No HV trip is observed during detector operation: thanks to the resistors protecting the THGEM segments and the MM pads, in case of occasional discharges, only current sparks are observed, which temporarily affect the local performance. The sparks in the two THGEM layers are fully correlated. The sparks observed in the MM are induced by the THGEM sparks. The restoration after a current spark is completed within 10 s and the current spark rate is typically 1/h/detector ($600 \times 600 \text{ mm}^2$). These figures result in totally negligible dead-time related to sparks.

The measured rate of ion backflow to the photocathode is at the 3% level. The electronics noise, substantially uniform over the detector surface, is at the 900 electrons equivalent level (r.m.s.).

The images generated in the photon detectors are clean and affected by very limited background (Fig. 3). The detector resolution in the measurement of the Cherenkov angle from single photoelectrons is 1.7-1.8 mrad r.m.s., fully matching the expectation (Fig. 4). The amplitude spectrum of the photoelectron signals is expected to be exponential. This is verified for pure photoelectron samples, obtained selecting hits contributing to ring images: the exponential behavior is present over more than two orders of magnitude (Fig. 5). The detector gain is extracted from a fit of the spectrum and it ranges between 13k and 14k. An electronic threshold of 3 times the noise level as measured pad by pad is applied to each read-out channel. The efficiency for single photoelectron detection is obtained from the gain and the threshold and it results higher than 80%. The noise contributing to the ring images can be estimated from the spectrum deviation from a pure exponential function at small amplitude and it is at the 10% level. A preliminary estimate of the number of detected photoelectrons per particle extrapolated to the saturation angle indicates 11 photoelectrons.

The high effective gain, the gain stability and the number of detected photoelectrons per ring satisfy all the prerequisite requirements to ensure effective hadron identification and stable performance with the novel RICH-1 photon detectors.

6. Future perspective

The future Electron-Ion Collider (EIC) [11] requires hadron identification at high momenta, a mission that can only be accomplished by RICH counters with an extended gas radiator. The use of RICHes in the setup of collider experiments implies specific challenges. The radiator cannot be too extended to limit the overall apparatus size, imposing the need to detect more photoelectrons per radiator unit length. The photon detectors have to operate in presence of magnetic field. A recent test-beam exercise has demonstrated the possibility to increase the number of detected photoelectrons by selecting the far UV range around 120 nm [12]. For this purpose, the RICH prototype has been operated window-less and CF_4 has been used at the same time as radiator gas and detector gas. Therefore, we have started an R&D program to match these specific requirements. It includes the exploratory study of a new option for the photoconverter: coating by hydrogenized nanodiamond powder [13].

7. Conclusion

The preliminary results obtained in the characterization of novel MPGD-based photon detectors, in particular high effective gain, gain stability and number of photons per ring, indicate that they will fully accomplish the mission of increasing the stability and efficiency of the photon detector system of COMPASS RICH-1. They also represent a technological achievement. In

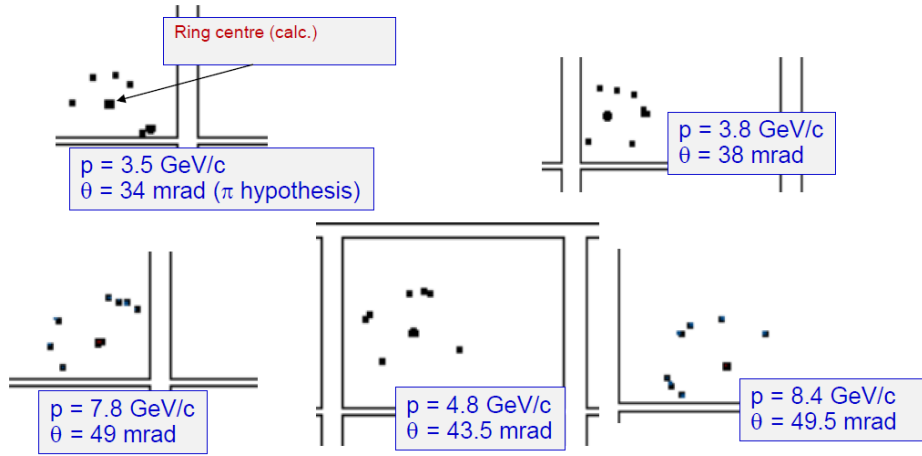


Figure 3. Images of hit pattern in the novel photon detectors. The center of the expected ring patterns is obtained from the reconstructed particle trajectories; the particle momentum and the expected Cherenkov angle in the pion hypothesis are also reported. No image elaboration or background subtraction is applied.

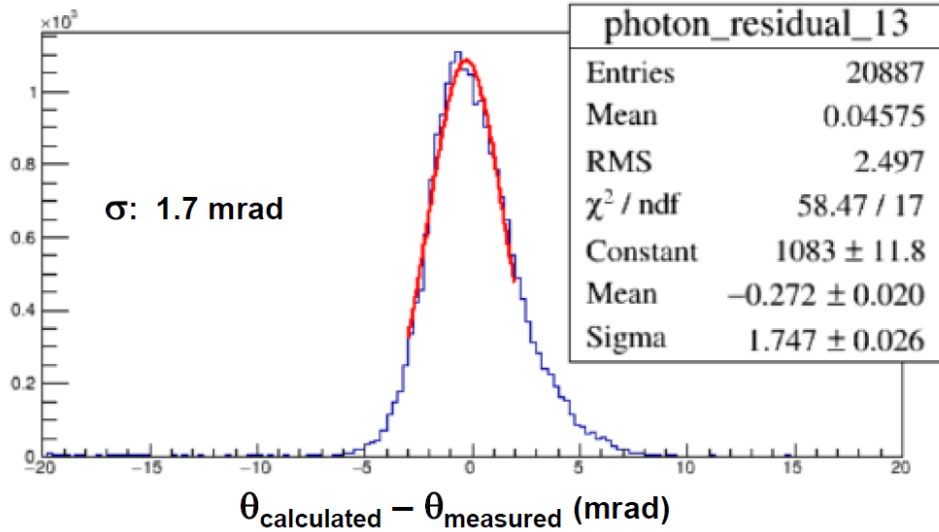


Figure 4. Distribution of the difference between the Cherenkov angle calculated from the reconstructed particle momentum and the Cherenkov angle provided by single detected photoelectrons; a sample of identified pions is used.

fact, for the first time in a running experiment, THGEMs are successfully used, single photon detection is accomplished by MPGDs, MPGDs are operated at gains larger than 10k.

We have offered indications that MPGD-based photon detectors have a mission to accomplish also in the future, in particular in the hadron physics sector.

Acknowledgments

The authors are grateful to the colleagues of the COMPASS Collaboration for continuous support and encouragement.

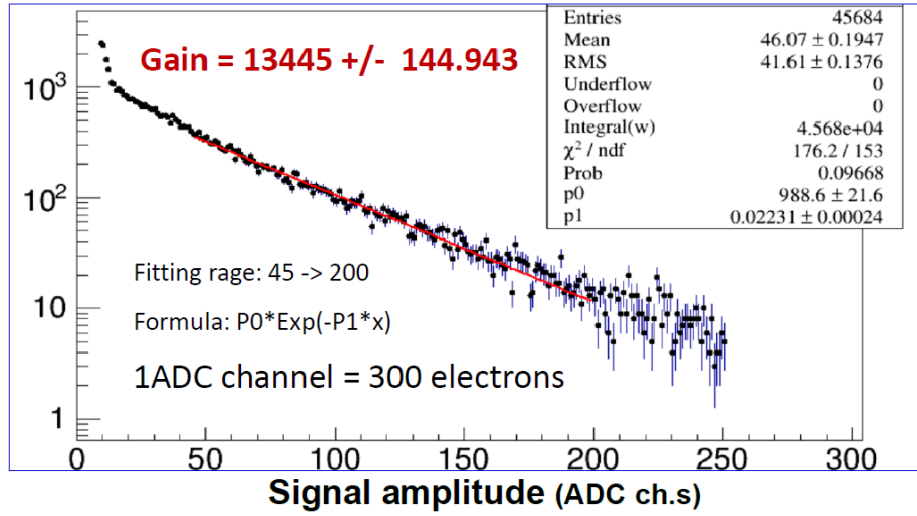


Figure 5. Amplitude distribution for a sample of hits contributing to ring Cherenkov images.

The use of the read-out system, originally designed and built for the MWPC with CsI photocathodes by the Munich and Saclay COMPASS groups, is a crucial ingredient for the successful performance of the MPGD-based photon detectors in COMPASS RICH.

This work is partially supported by the H2020 project AIDA-2020, GA no. 654168. J. Agarwala and Triloki are supported by ICTP TRIL fellowships.

References

- [1] E. Albrecht, et al., Status and characterisation of COMPASS RICH-1, Nucl. Instrum. Meth. A553 (2005) 215; P. Abbon et al., Read-out electronics for fast photon detection with COMPASS RICH-1, Nucl. Instrum. Meth. A587 (2008) 371; P. Abbon et al., Design and construction of the fast photon detection system for COMPASS RICH-1, Nucl. Instrum. Meth. A616 (2010) 21; P. Abbon et al., Particle identification with COMPASS RICH-1, Nucl. Instr. and Meth. A631 (2011) 26.
- [2] The COMPASS Collaboration, P. Abbon et al., The COMPASS experiment at CERN, Nucl. Instrum. Meth. A577 (2007) 455; the COMPASS Collaboration, P. Abbon et al., The COMPASS setup for physics with hadron beams, Nucl. Instrum. Meth. A779 (2015) 69.
- [3] M. Alexeev et al., The quest for a third generation of gaseous photon detectors for Cherenkov imaging counters, Nucl. Instrum. Meth. A610 (2009) 174; M. Alexeev et al., THGEM based photon detector for Cherenkov imaging applications, Nucl. Instrum. Meth. A617 (2010) 396; M. Alexeev et al., Micropattern gaseous photon detectors for Cherenkov imaging counters, Nucl. Instrum. Meth. A623 (2010) 129; M. Alexeev et al., Development of THGEM-based photon detectors for Cherenkov Imaging Counters, 2010 JINST 5 P03009; M. Alexeev et al., Progress towards a THGEM-based detector of single photons, Nucl. Instrum. Meth. A639 (2011) 130; M. Alexeev et al., Detection of single photons with ThickGEM-based counters, 2012 JINST 7 C02014; M. Alexeev et al., Detection of single photons with THickGEM-based counters, Nucl. Instrum. Meth. A695 (2012) 159; M. Alexeev et al., Development of THGEM-based Photon Detectors for COMPASS RICH-1, Physics Procedia 37 (2012) 781; M. Alexeev et al., THGEM-based photon detectors for the upgrade of COMPASS RICH-1, Nucl. Instrum. Meth. A732 (2013) 264; M. Alexeev et al., Ion backflow in thick GEM-based detectors of single photons, 2013 JINST 8 P01021; M. Alexeev et al., Status and progress of novel photon detectors based on THGEM and hybrid MPGD architectures, 2013 JINST 8 C12005; M. Alexeev et al., Progresses in the production of large-size THGEM boards, 2014 JINST 9 C03046; M. Alexeev et al., MPGD-based counters of single photons developed for COMPASS RICH-1, 2014 JINST 9 C09017; M. Alexeev et al., Status and progress of the novel photon detectors based on THGEM and hybrid MPGD architectures, Nucl. Instrum. Meth. A766 (2014) 133; M. Alexeev et al., MPGD-based counters of single photons for Cherenkov imaging counters, PoS (TIPP2014) 075; M. Alexeev et al., The gain in Thick GEM multipliers and its time-evolution, 2015 JINST 10 P03026;

- M. Alexeev et al., Status of the development of large area photon detectors based on THGEMs and hybrid MPGD architectures for Cherenkov imaging applications, Nucl. Instrum. Meth. A824 (2016) 139.
- [4] L. Periale et al., Detection of the primary scintillation light from dense Ar, Kr and Xe with novel photosensitive gaseous detectors, Nucl. Instrum. Meth. A478 (2002) 377; P. Jeanneret, Time Projection Chambers and detection of neutrinos, PhD thesis, Neuchatel University, 2001; P.S. Barbeau et al, Toward coherent neutrino detection using low-background micropattern gas detectors IEEE NS-50 (2003) 1285; R. Chechik et al, Thick GEM-like hole multipliers: properties and possible applications, Nucl. Instrum. Meth. A535 (2004) 303.
 - [5] Y. Giomataris et al., MICROMEGAS: a high-granularity position-sensitive gaseous detector for high particle-flux environments, Nucl. Instrum. Meth. A376 (1996) 29.
 - [6] I. Giomataris et al., Micromegas in a bulk, Nucl. Instrum. Meth. A560 (2006) 405.
 - [7] [6] M. J. French, et al., Nucl. Instrum. and Meth. A 466 (2001) 359.
 - [8] P. Abbon, et al., Nucl. Instrum. and Meth. A 589 (2008) 362.
 - [9] S.S. Dasgupta, "Particle identification with the Cherenkov imaging technique using MPGD based photon detectors for physics at COMPASS Experiment at CERN", University of Trieste, April 2017.
 - [10] F. Paschen, Über die zum Funkenübergang in Luft, Wasserstoff und Kohlensäure bei verschiedenen Drucken erforderliche Potentialdifferenz, Annalen der Physik 273 (1889) 69.
 - [11] A. Accardi et al., Electron-Ion Collider: The next QCD frontier, Eur. Phys. J. A52 (2016) 268.
 - [12] M. Blatnik et al., Performance of a Quintuple-GEM Based RICH Detector Prototype, IEEE NS 62 (2015) 3256.
 - [13] L. Velardi, A. Valentini, G. Cicala, UV photocathodes based on nanodiamond particles: Effect of carbon hybridization on the efficiency, Diamond and Related Materials 76 (2017) 1.